

The Performance of an AGMD Unit Coupled with a Water Solar Collector the Experimental Validation for Desalination of Seawater

Mokhless Boukhriss^{1*} and Habib Ben Bacha^{1,2}

¹Laboratory of Electromechanical Systems, National School of Engineers, Sfax, Tunisia

²College of Engineering, Prince Sattam Bin Abdul-Aziz University, Alkharj, Kingdom of Saudi Arabia

Abstract

Our work consists in presenting the results of an invention for a membrane distillation system coupled to an efficient and robust water solar collector which produces potable water with high quality and a small percentage of brackish discharge independent of salinity of the water source. The air gap membrane distillation (AGMD) model for the modules has been developed. This model is based on mathematical equations that describe the heat and mass transfer mechanisms of a single-stage AGMD process. It can simulate AGMD modules in regimes. The theoretical model was validated using in AGMD under different operating conditions and parameters. The predicted water vapor flux was compared to the flux measured at five different feed water temperatures, two different feed water salinities. The model was then used to study and analyze the parameters that have significant effect on scaling-up the AGMD process such as the effect of increasing the membrane length, and feed and coolant flow rates. The model was also used to analyze the maximum thermal efficiency of the AGMD process

Keywords: Desalination; Membrane distillation; Air gap membrane distillation; Solar energy; Coupling

Abbreviations: A: area (m²); B: effective absorptivity; Cp: heat capacity (J/kg K); D: diffusion coefficient (m²/s) ; Fj : objective function; H: height (m); HVL: heat transfer rate of phase change (J/m²s); h: heat transfer coefficient (W/m²K); I: intensity of solar radiation (W/m²); K: thermal conductivity (W/m K); Kc: proportional gain; Ku: ultimate gain; k: mass transfer coefficient (m/s); L: length (m); M: mass (kg); Mw: molecular weight of water kg/kmol); mf: fluid flowrate (kg/s); mf,c: fluid collector flowrate (kg/s); N: Mass flux (kmol/m²s); OP: controller output; P: pressure (Pa); Q: heat transfer rate (J/s); QN: sensible heat transfer rate (J/s); R: gas constant (J/kmol K); S: collector absorber surface area (m²); Si: stream number I; T: temperature (K); U: overall heat transfer coefficient of the heat exchanger (W/m²K); U': overall heat loss coefficient between the collector absorber and the surroundings (W/m²K); W: width (m); DHvap: heat of vaporization (J/kmol); D: thickness (m); e: membrane porosity; m: viscosity (kg/m s); r: density (kg/m³); s: membrane tortuosity; sl: integral time (s); su: ultimate period (s); L: liquid; G: gas; Sat: saturated; AG: air gap ; A: Ambient ; Air: air ; Avg: average; c: solar collector; CL: cold liquid; CONL: condensate liquid; F: condensing film surface in the air gap; F: circulation fluid in the solar collector; fh: circulation fluid between the coil and the heat exchanger; fs: circulation fluid between the internal coil and the solar; Tf: fluid temperature (K); Tc: collector temperature (K); GM: gas in the membrane; HL: hot liquid; MD: membrane module; MEM: membrane; MET: metal; Nu: Nusselt number; Pr: Prandtl number; Re: Reynolds number; T: total; w: water; wa: watereair;

Introduction

Membrane distillation is a separation process that involves transport of water vapour through porous hydrophobic membranes. A variety of methods may be employed to impose this vapour pressure difference. In the present work, the air gap membrane distillation method (AGMD) is considered. The principal advantage of AGMD against other configurations of membrane distillation arises from the possibility to condensing the permeate vapours on a cold surface rather than directly in a cold liquid. In this configuration, the mass transfer steps involve movement within the liquid feed toward

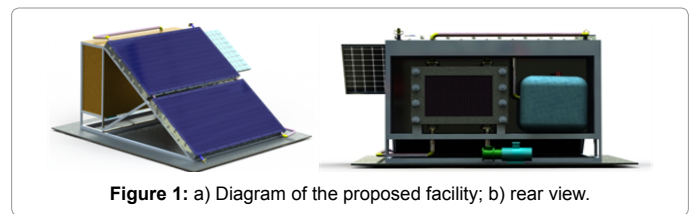


Figure 1: a) Diagram of the proposed facility; b) rear view.

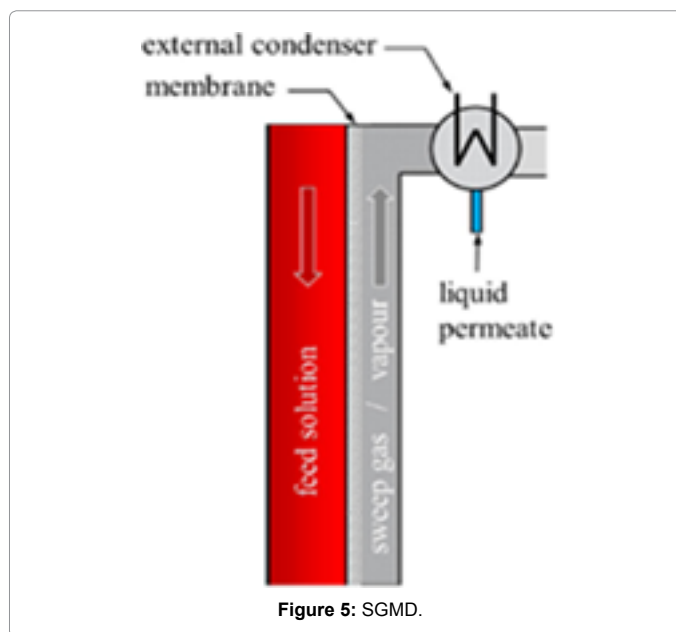
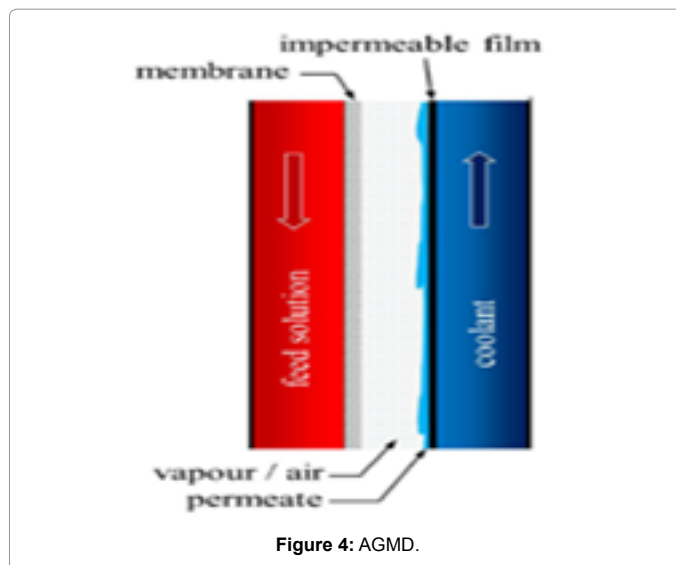
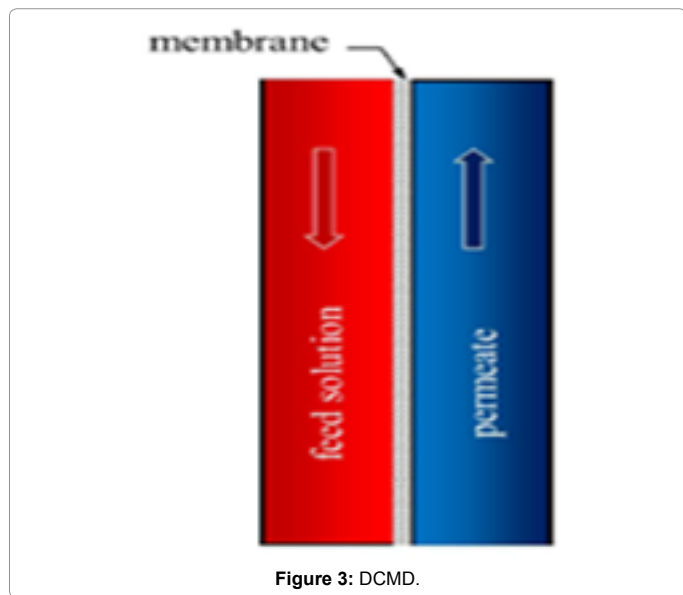
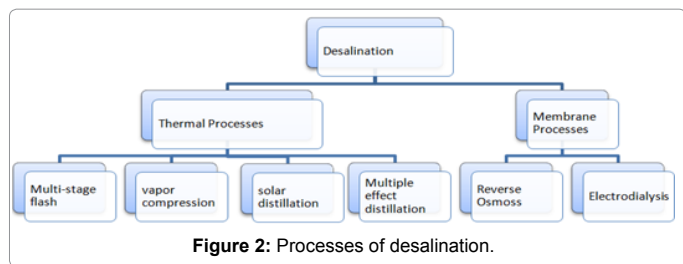
the membrane surface, evaporation at the membrane interface and transport of the vapour through the membrane pores and air gap prior to condensation. So, the separation mechanism of membrane distillation and its performance is based on vapour-liquid equilibrium. The driving force of the process is supplied by the vapour pressure difference caused by the existing temperature difference between the liquid-vapour interfaces. The benefits of membrane distillation over conventional distillation processes are found in the lower operating temperatures and pressures that reduce the equipment surface and costs, the compact modules and the possibility of overcoming corrosion problems by using plastic equipment. The lower operating temperatures can use available energy sources such as solar and geothermal energies or waste energy in industrial processes. That is why transmembrane evaporation applied to the desalination of seawater is a very promising technology to reduce the production costs of water from fresh water sources [1] (lakes, solar pond, etc.). However, at this moment little knowledge is available about the

***Corresponding author:** Mokhless Boukhriss, Laboratory of Electromechanical Systems National School of Engineers, Sfax, Tunisia, Tel: +216 74 274 088; E-mail: mokhlessisset@yahoo.fr

Received January 24, 2018; Accepted April 18, 2018; Published April 25, 2018

Citation: Boukhriss M, Bacha HB (2018) The Performance of an AGMD Unit Coupled with a Water Solar Collector the Experimental Validation for Desalination of Seawater. J Fundam Renewable Energy Appl 8: 256. doi:10.4172/20904541.1000256

Copyright: © 2018 Boukhriss M, et al. This is an open-access article distributed under the terms of the Creative Commons Attribution License, which permits unrestricted use, distribution, and reproduction in any medium, provided the original author and source are credited.



optimal design of such a transmembrane evaporation process. In fact, the coupling and non-linearity of the equations, the interaction between the flow and the thermal plume in the cavity and the complicated geometries involved have forced experimental solutions. So, the evident lack of data for thermal and dynamic interactions in natural convection within the cavity prompted the present study. This work presents a model for preliminary design calculations that is used to evaluate the effect of the main design parameters in the transmembrane evaporation module performance for water desalination. Developing mathematical models for prediction of membrane separation processes is an important tool in the field of membrane science and technology. The models play a meaningful role in simulation and optimization of membrane systems leading to efficient and economical designs of separation processes [1–3]. This paper presents the modeling of phenomena (mass and heat transfers) and the experimental and simulated results of the parametric study of an installation of type PTFE on the pilot scale (500 L) is shown in Figure 1.

Materials and Methods

The different desalination methods

Figure 2 illustrates the desalination techniques classified in two broad categories: membrane processes and thermal processes. The processes acting on the chemical bonds and processes are being performed by phase change. A method for separating salt water desalination in two parts: fresh water containing a low concentration of dissolved salts and concentrate brine. This process is energy-consuming various desalination techniques have been implemented over the years on the basis of the available energy [4,5].

Principles of MD: MD is a thermal process in which water vapor is transported through a hydrophobic porous membrane. The liquid phase to be treated must be kept in contact with one face of the membrane without penetrating the pores unless the trans membrane pressure is greater than the inlet pressure. The hydrophobicity of the membrane prevents the liquid entering the pores due to the surface tension. Thus, liquid/vapor interfaces are created in the vicinity of the pores.

Different configurations of MD

Direct contact membrane distillation (DCMD): A colder aqueous solution than the feed solution is maintained in direct contact with the permeate membrane (Figure 3). In this case, the transmembrane temperature difference induces a vapor pressure difference. Consequently, the volatile molecules evaporate at the liquid / vapor interface of the feed and condensate at the liquid / vapor interface of the colder permeate.

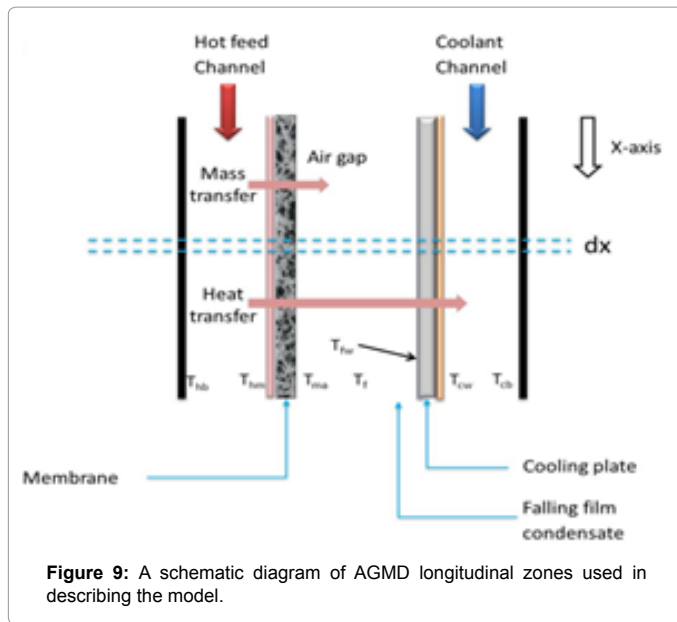


Figure 9: A schematic diagram of AGMD longitudinal zones used in describing the model.

of the hot feed flow, and each small element is assumed to have a length of dx and a constant width W . Moreover, the mathematical model calculations were simplified according to the following assumptions:

- The system is at steady state condition.
- The hot and cold fluids are assumed to flow in the x direction only.
- The pressure inside the air gap is constant (no pressure drop along the air gap zone).
- The condensation on the cooling plate is film-wise and the thickness of the falling film inside the air gap is small in comparison with the width of the air gap.
- Within the air gap, there is no bulk velocity of the air-vapor mixture. Heat is transferred by conduction while mass is transferred through diffusion.
- Pure water vapor is only transported through membrane pores.
- There is no heat being exchanged with the surrounding.

The main components are the solar collector and the MD module, but you can add a heat exchanger with a slack storage if we will work day and night. The MD module is featured with a design of energy [4-6] recovery. The System's performance is determined by the profiles of solar radiation, the design of individual system components, component integration, the business model and the control strategy. Modeling and control methods of solar desalination, Ben Bacha et al. [7] and Roca et al. [8] presented studies for a solar cycle system condensation and evaporation multiple hybrid fossil fuel powered solar distillation system, respectively. Both groups have developed reduced process for integrating their control algorithms proposed on the basis of linear technology control and feedback linearization technique, models respectively. Due to the intermittent and unpredictable nature of solar radiation, the steady state operation of the solar desalination process is not easy to achieve and the application of modern control algorithms is difficult. The purpose of this study is to develop a dynamic model including models for key components, and the latter to investigate the

overall system optimization. The model is built on platform [9], which allows the analysis and control system design.

The hot fluid and hot fluid is against the current. For simplicity, seawater is used, along with hot and cold fluids in the model [10,11]. The purpose of this study is to investigate the optimization and control of the entire system, this simplification will not cause significant differences in the test results. The mass transfers resistance of the hot fluid side which is insignificant in a previous analysis [12] to the hollow fiber module. Transferring the mass flow is determined by taking into account the mass transfer resistance in the gap and membrane. However, the heat transfer resistance of the whole layers is taken into account. Mass and energy flows for all layers, including the hot fluid, the membrane gap, a cold fluid and metal sheet are illustrated in Figure 10, the model equations are summarized below.

The mass balances:

$$\frac{dm_{f,HL}}{dz} = -N_{GM,w}L_wM_w \quad (1)$$

$$\frac{dm_{f,CONL}}{dz} = -N_{AG,w}L_{MD}M_w \quad (2)$$

$$N_{GM,w} = N_{AG,w} \quad (3)$$

Balancing the energy:

$$\frac{\partial T_{HL}}{\partial t} = -W_{MD} \left[\frac{m_{f,HL}}{M_{HL}} \frac{\partial T_{HL}}{\partial z} + \frac{L_{MD}}{M_{HL}C_{p,HL}} (h_{HL} + N_{GM,w}C_{p,w}^L M_w) \times (T_{GM(1)} - T_{GM(2)}) \right] \quad (4)$$

$$\frac{\partial T_{CL}}{\partial t} = -W_{MD} \left[\frac{m_{f,CL}}{M_{CL}} \frac{\partial T_{CL}}{\partial z} + \frac{L_{MD}h_{CL}}{M_{CL}C_{p,CL}} (T_{MET(2)} - T_{CL}) \right] \quad (5)$$

$$Q_{HL} + Q_{N,HL} - H_{VL,HL} = Q_{GM} + Q_{N,GM} \quad (6)$$

$$Q_{GM} + Q_{N,GM} = Q_{AG} + Q_{N,AG} \quad (7)$$

$$Q_{AG} + Q_{N,AG} + H_{VL,AG} = Q_{CONL} + Q_{N,CONL} \quad (8)$$

$$Q_{MET} = Q_{CONL} + Q_{N,CONL} \quad (9)$$

$$Q_{MET} = Q_{CL} \quad (10)$$

Mass fluxes:

$$N_{GM,w} = \frac{k_{GM,w}}{RT_{GM,arg}} (P_{GM(1),w}^{sat} - P_{AG(1),w}^{sat}) \quad (11)$$

$$N_{AG,w} = \frac{k_{GM,w}}{RT_{arg}P_{In,air}\delta_{AG}} (P_{AG(1),w}^{sat} - P_{F,w}^{sat}) \quad (12)$$

Heat fluxes:

$$Q_{HL} = h_{HL} (T_{HL} - T_{GM(1)}) \quad (13)$$

$$Q_{GM} = [\varepsilon h_{GM} + (1 + \varepsilon)h_{MEM}] (T_{GM(1)} - T_{GM(2)}) \quad (14)$$

$$Q_{AG} + Q_{N,AG} = h_{AG} \frac{\theta}{e^{-\theta}} (T_{GM(2)} - T_F) \quad (15)$$

$$A_{vec} = NC_p / h$$

$$Q_{CONLL} = h_{CONL} (T_F - T_{MET(1)}) \quad (16)$$

$$Q_{MET} = h_{MET} (T_{MET(1)} - T_{MET(2)}) \quad (17)$$

$$Q_{CL} = h_{CL} (T_{MET(2)} - T_{CL}) \quad (18)$$

$$Q_{N,HL} = N_{GM,N} C_{p,w}^L (T_{HL} - T_{GM(1)}) \quad (19)$$

$$Q_{N,GM} = N_{GM,N} C_{p,w}^L (T_{GM(1)} - T_{GM(2)}) \quad (20)$$

$$Q_{N,CONL} = N_{AG,w} C_{p,w}^L (T_F - T_{MET(1)}) \quad (21)$$

$$H_{VL,HL} = H_{GM,w} \Delta H_{vap,w} \quad (22)$$

$$H_{VL,AG} = H_{AG,w} \Delta H_{vap,w} \quad (23)$$

The heat transfer coefficients for hot and cold fluid sides are estimated using the correlations reported by Schock and Miquel for the module flat plate wound membrane.

$$Nu = 0.065 \cdot Re^{0.875} \cdot Pr^{0.25} \quad (24)$$

For the condensing heat transfer to the film, the following relationship is employed [13]:

$$h_{CONL} = 0.943 \left[\frac{\rho_w^L (\rho_w^L - \rho_w^V) g \Delta H_{vap,w} K_w^L}{L_{MD} \mu_w (T_{CONL} - T_{MET})} \right] \quad (25)$$

Results and Discussion

Simulation for membrane distillation unit

Model validation at different operating parameters: The first

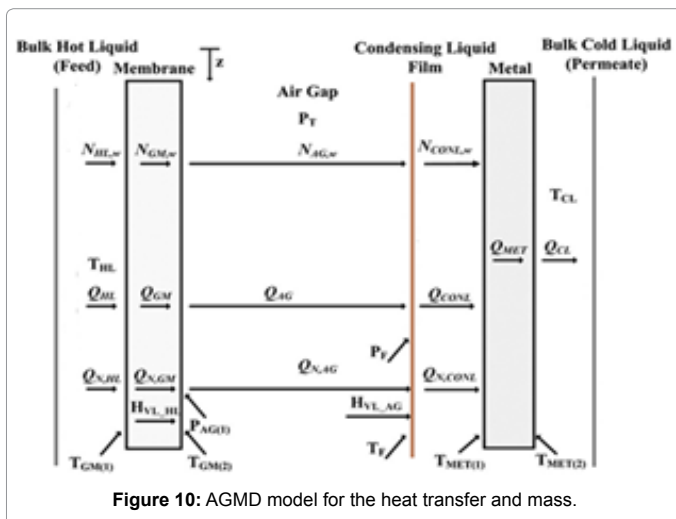


Figure 10: AGMD model for the heat transfer and mass.

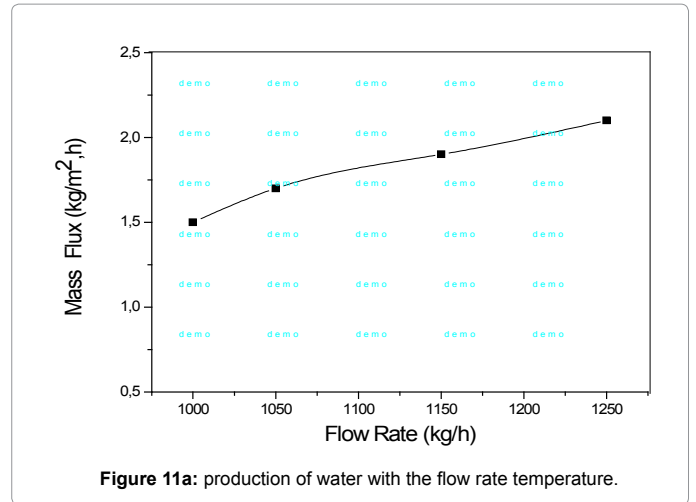


Figure 11a: production of water with the flow rate temperature.

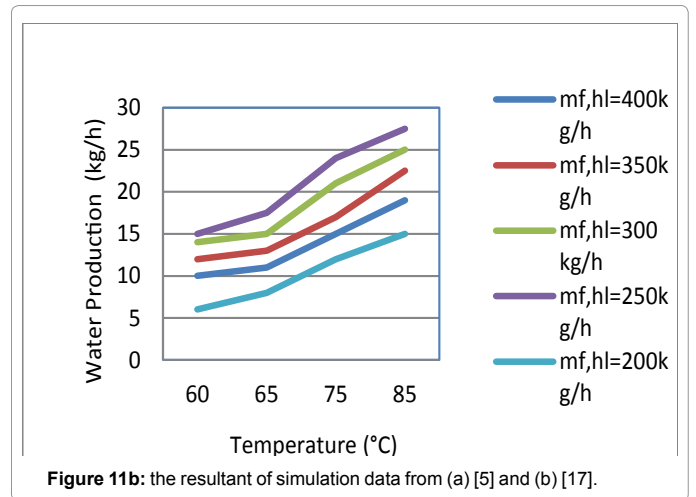


Figure 11b: the resultant of simulation data from (a) [5] and (b) [17].

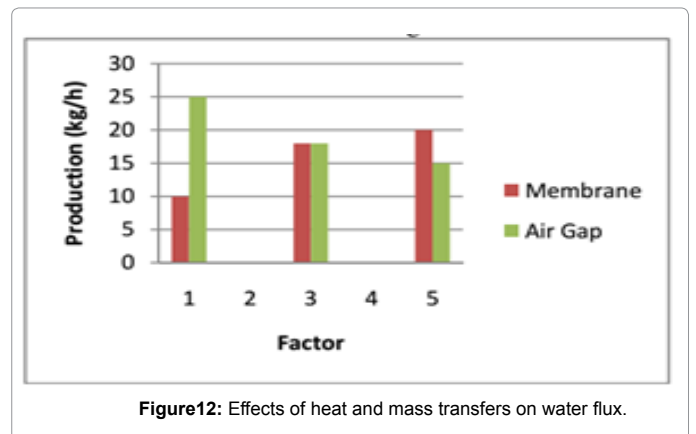


Figure 12: Effects of heat and mass transfers on water flux.

set of experiments was conducted to test the reproducibility and to determine the experimental errors. The measured water vapor flux at different feed water temperatures was repeatable and the variation in flux was a maximum of $\pm 0.12 \text{ kg/m}^2 \cdot \text{hr}$ (2%). The mathematical model results were then validated against different experimental data (Figure 11a and 11b).

Using AGMD model, effects of heat and mass of the membrane and the air gap are studied by varying the heat transfer coefficients and

mass simultaneously by a factor of 0.1 or 10. The results are shown in Figure.12.

Model validation at different operating parameters: The first set of experiments was conducted to test the reproducibility and to determine the experimental errors. The measured water vapor flux at different feed water temperatures was repeatable and the variation in flux was a maximum of $\pm 0.12 \text{ kg/m}^2 \cdot \text{hr}$ (2%). The mathematical model results were then validated against different experimental data. Figure 13 shows a comparison between the predicted mass fluxes and the measured water vapor fluxes for a range of deionized feed water temperatures (40°C-80°C). The model predicted an exponential behavior of the AGMD flux as a function of feed water temperature. Such behavior is not only supported by our experimental data but also reported in published AGMD literature [14-17]. However, the validity of the mathematical model should not be judged based on predicting the trend of the process but also on how closely it predicts the absolute experimental data. Our current purpose of developing this model is to utilize it as a tool for further analyzing the AGMD process and for scale-up. Such a goal may require relaxed a criterion toward which we may judge the validity of our module. Nonetheless, the prediction of the model was within the range of the experimental error.

To validate the model further we replaced the deionized water (feed) with Red Sea water to see how the model predicts the water vapor flux for a seawater salinity of 4.2 wt%. The distillate conductivity was continuously measured to check for any pore wetting that may took place and the distillate conductivity was always below $20 \mu\text{S}$. As shown in Figure 14 the predicted water vapor flux was also within the range of experimental error.

The effect of air gap width was also investigated. As shown in Figure 15 the model predicted decay in flux as the air gap increased. However, the model predictions for water vapor flux at different air gap widths was not as good as were the predictions for variations in feed temperature. Analysis of the results showed that the water vapor flux was very sensitive to the change of air gap width, especially when it is very small. A reduction in air gap width results in higher production capacity and higher errors. These errors are more significant when the air gap width is very small. Therefore, any small error in measuring the gap width (i.e., by 0.1 mm) will affect the water vapor flux significantly. The error of our measurements to the gap width was about $\pm 0.5 \text{ mm}$. Our investigation showed that this was due to the deformation of the

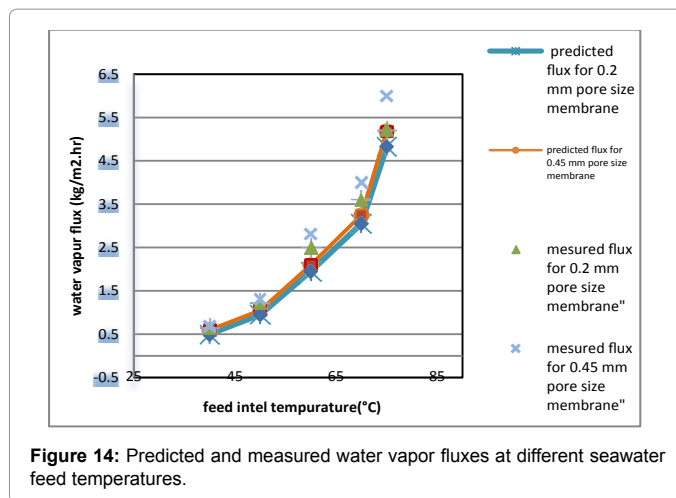


Figure 14: Predicted and measured water vapor fluxes at different seawater feed temperatures.

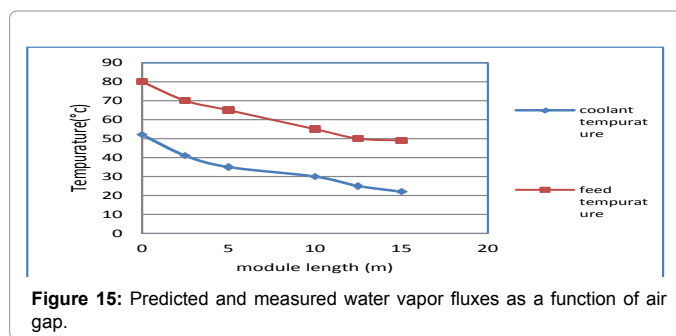


Figure 15: Predicted and measured water vapor fluxes as a function of air gap.

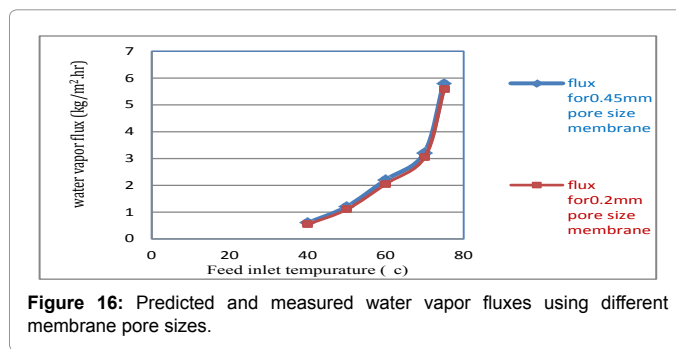


Figure 16: Predicted and measured water vapor fluxes using different membrane pore sizes.

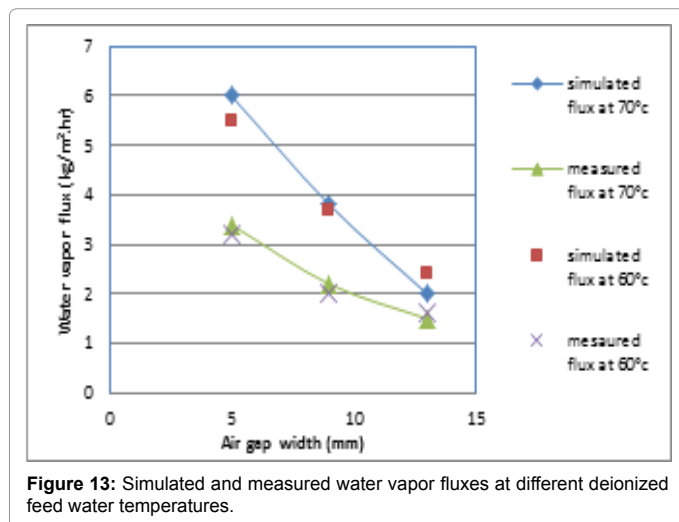


Figure 13: Simulated and measured water vapor fluxes at different deionized feed water temperatures.

parafilm tape used in sealing the module. Further experimental tests with a modified module are required in the future to better evaluate the model prediction at small air gap width.

Finally, the model was validated against experimental data using different membrane pore sizes. The model prediction was good enough ($\pm 10\%$), although it didn't predict well the data (15%) at feed temperature of 70°C for the 0.45 μm membrane (Figure 16). In this region the flux is increasing significantly as feed temperature is increased, so variations in the inlet temperature will have a larger effect on the measured flux compared to measurements at lower feed temperatures, and the error of 15% appears reasonable.

SEM images and membrane properties

The SEM observation indicated that the PDPE membrane (Table 1) studied is characterized by a foam structure and is symmetrical. Some

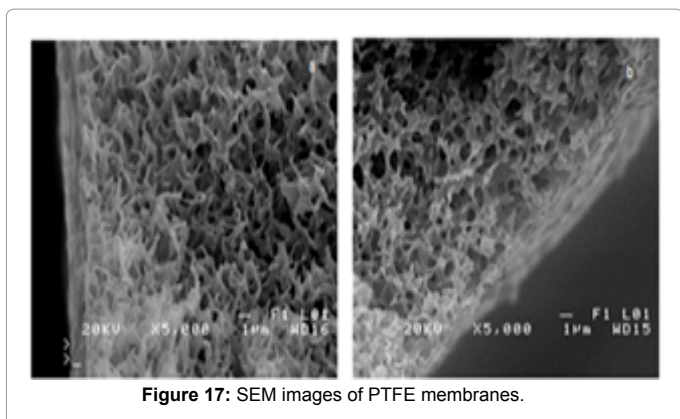


Figure 17: SEM images of PTFE membranes.

differences in pore size occurred only on the outer surface (Figure 17). The maximum pore size observed on the inner membrane surface did not exceed a few microns.

Mass transfer in the MD process is diffuse. Therefore, the permeate flux is strongly affected by the wall thickness of the membrane and the pore diameter. The results of the study confirmed that the type of membrane used has a significant influence on the efficiency of the MD process (Figure 15).

Given the membranes with similar wall thickness, a higher flux was obtained, having a larger pore size in a membrane. Molecular diffusion and Knudsen influence mass transfer in the MD process, therefore, the permeate flux increases with an increase in pore diameter.

Conclusion

The mathematical model of a membrane module was developed from mass equations and heat transfer. The model calculations were based on the division of the AGMD module in different longitudinal areas. Normal for these areas of the module was cut into small cells. The mass and energy equation were applied to these slices and resolved by iterative procedures. The model has been validated under different conditions such as water temperatures, nutrition salinity, membrane pore sizes, and gap widths.

The model used in the analysis of complex and interdependent AGMD processes, which are essential elements for the extension of processes. The current analysis of the residence time in the indoor module AGMD is very important for the extension of processes because it has a direct effect on the process flow and its thermal efficiency. The flux decreases as the length of the membrane increases and increases with flow rate.

In addition, the efficiency of the process increases so that the surface of the membrane that increases the AGMD processes to operate at low temperature difference across the membrane. The effect of the type of flow is more visible with the variations of the flow rates than with the variation of the temperature of supply of the hot fluid. This effect

disappears when the thickness of the air gap is high. The maximum permeate flux obtained was $7.4 \text{ kg} / \text{m}^2 \text{ h}$ with a fluid temperature of 80°C ., air gap of 1.04 mm and hot and cold flow rates of 5 l / min. This work reveals that even at the low hot fluid supply temperature of 25°C ., the AGMD configuration is capable of producing desalinated water. This aspect of the process may be useful in coupling with low temperature heat sources.

The membrane was then characterized by the SEM and FTIR technique to locate the presence of salt on the membrane.

Other tests will be carried out soon on the long-term use and the clogging effect of the membrane which is the main lock to the development of this kind of desalination technique.

References

1. Lloyd DR, Lawson KW (1997) Membrane distillation. *J Memb Sci* 124: 1-25.
2. Bourawi MS, Ding Z, Ma R, Khayet M (2006) A framework for better understanding membrane distillation separation process. *J Memb Sci* 285: 4-29.
3. Kalogirou SA (2005) Seawater desalination using renewable energy sources. *Progr Energy Combust Sci* 31: 242-281.
4. Banat F, Jwaied N, Rommel M, Koschikowski J, Wiegghaus M (2007) Performance evaluation of the "large SMADES" autonomous desalination solar-driven membrane distillation plant in Aqaba, Jordan. *Desalination* 217: 17-28.
5. Banat F, Jwaied N, Rommel M, Koschikowski J, Wiegghaus M (2006) Desalination by a "compact SMADES" autonomous solar-powered membrane distillation unit. *Desalination* 217: 29-37.
6. Van Medevoort J, Jansen A, Hanemaaijer JH, Dotremont C, Nelemnas B, et al. (2008) Memstill: Seawater desalination a solution to water scarcity.
7. Ben Bacha H, Bouzguenda M, Damak T, Abid MS, Maalej AY (2000) A study of a water desalination station using the SMCEC technique: production optimization. *Renewable Energy* 21: 523-536.
8. Roca L, Berenguel M, Yebra L, Alarcón DC (2008) Preliminary modeling and control studies in AQUASOL project. *Desalination* 222: 466-473.
9. <https://www.aspentech.com/en/products/pages/aspem-custom-modeler>
10. Ben Bacha H, Damak T, Bouzguenda M, Maalej AY, Ben Dhia H (2003) A methodology to design and predict operation of a solar collector for a solar-powered desalination unit using the SMCEC principle. *Desalination* 156: 305-313.
11. Avlonitis S, Hanbury WT, Ben Boudinar M (1993) Spiral wound modules performance an analytical solution: part II. *Desalination* 89: 227-246.
12. Chang H, Liao JS, Ho CD, Wang WH (2009) Simulation of membrane distillation modules for desalination by developing user's model on Aspen Plus platform. *Desalination* 249: 380-387.
13. Holman JP (1989) Heat transfer. McGraw-Hill, New York.
14. Koschikowski J, Wiegghaus M, Rommel M (2003) Solar thermal-driven desalination plants based on membrane distillation. *Desalination* 156: 295-304.
15. Schock G, Miquel A (1987) Mass transfer and pressure loss in spiral wound modules. *Desalination* 64: 339-352.
16. Chen CX, Yu LX, Dai TY (1996) Review of new membrane and membrane process. *Technology of Water Treatment* 22: 307-313.
17. Liu LY, Ding CW, Chang LJ (2008) Progress in membrane separation enhanced by ultrasound. *Chemical Industry and Engineering Progress* 27: 32-37.